FATIGUE CRACK GROWTH MONITORING OF AN ALUMINUM JOINT STRUCTURE

C. J. Lissenden[1], H. Cho[1], and C. S. Kim[1]

[1]Department of Engineering Science and Mechanics, The Pennsylvania State University, University Park, PA 16802

ABSTRACT. The detection, location, and sizing of a fatigue crack emanating from a fastener hole in an aluminum plate is investigated. Two linear arrays of surface mounted piezoelectric disk transducers send and receive ultrasonic guided waves that are transmitted, reflected, and scattered by both the joint geometry and the fatigue crack. A tomography algorithm is used to detect and locate the crack. Amplitude ratio and signal difference coefficients are explored as candidate features to size the crack, which is necessary for reliability and remaining life calculations. Both of these features are quite sensitive to fatigue crack lengths as small as 0.13 of the hole diameter.

Keywords: Structural Health Monitoring, Lamb Waves, Fatigue Cracks
PACS: 43.20.Gp, 43.20Mv, 46.40Cd

INTRODUCTION

Some initial results are presented from a project aiming to link guided wave ultrasonic technology (GWUT) with probabilistic fatigue crack growth modeling. Both phased array beam steering using the pulse-echo method [1] and tomography from an inward-looking array of transducers using the pitch-catch method [2] have been demonstrated recently for damage detection in plate-like structures. Structural health monitoring (SHM) using GWUT will provide a current damage state estimate for probabilistic fatigue crack growth modeling making possible condition based maintenance. The damage state estimate must include the full SHM hierarchy [3] of detection, location, classification, and extent in order to predict future damage states and the reliability of the structure. Furthermore, the project intends to consider a complex built-up plate structure, which is common in the aircraft industry. Experiments are planned for an aluminum alloy double lap joint having five fasteners. The experiments will include cyclic loading to initiate and propagate fatigue cracks as well as GWUT SHM to characterize the current damage state. Training data are necessary to determine the extent of damage (fatigue crack location and size). This paper presents results from experiments on aluminum plates with a hole or multiple holes. Both loading-induced fatigue cracks and electric discharge machined slots are employed to provide training data.

Fatigue crack growth is a stochastic process that should be represented by a probabilistic model. The Paris law (or similar variant thereof) can be used to advance the fatigue crack with cycling and the method recently presented by Kulkarni et al. [4] can be employed to estimate reliability, or more specifically, the probability that a fatigue crack will go undetected in all monitoring interrogations. In order to determine reliability, the probability of detecting a crack for a prescribed length range must be known. Moreover, the reverse analysis can be performed for a prescribed reliability and a monitoring protocol; thus, it is possible to determine the minimum probability of detection for a fatigue crack at this location. These modeling results will be presented in a future publication.

THEORY

Surface bonded transducers are used to actuate and sense Lamb waves in a plate specimen. The dispersion curves for a 2 mm thick aluminum plate are shown in Figure 1 and the central frequency of the transducers is marked. Since the transducers operate in a radial vibration mode for this frequency mode, they will excite the predominantly in-plane S0 mode more so than the A0 mode.

Once the current fatigue crack size is estimated and represented by a probability density function (PDF) the Paris law can be used to determine the crack length descriptors after a prescribed number of cycles. Future reliability is then quantified by determining the probability that the projected future fatigue crack is less than a critical value. Provided that the probability of detection (POD) curve for the hot spot monitoring method is known, the effect that monitoring has on the probability (Pr) that a crack larger than a prescribed critical size is not detected by the SHM system is:

$$\Pr\left(a_N > a_{cr}; N > N_n; ND\right) = F\left(f_0, a_{cr}, N, N_i, \xi_j, Y, POD\right) \quad (1)$$

where a_N is the crack length at cycle N, a_{cr} is the critical crack length, N_i (for i=1 to n) are the cycles when monitoring is performed, ND means 'not detected', f_0 is the initial PDF, ξ_j are material parameters for fatigue crack growth, and Y is the nondimensional crack geometry factor. Cobb et al. [5] discuss determination of POD for ultrasonic SHM systems. A specific form of this equation is given by Kulkarni et al. [4] and enables determination of an optimal SHM strategy in terms of monitoring schedule, monitoring POD, and desired reliability. From a practical standpoint, only the monitoring schedule in the off-board protocol is interesting, as on-board monitoring is expected to be continuous. Finally, it is recognized that the POD depends on the number and placement of sensors as well as other factors.

EXPERIMENT

Fatigue cracks and wire EDM slots were seeded in 6061-T6 aluminum alloy plates 2 mm thick and having 1 or 5 open fastener holes 12.7 mm in diameter. Surface mounted piezoelectric disk transducers (6.4 mm diameter and 1.0 mm thick) having a 350 kHz center frequency actuate and sense Lamb waves in the plate. The phase velocity and group velocity dispersion curves are shown in Figure 1. Five-cycle Hanning windowed tone burst signals (300 V, 30 dB gain, 10 dB attenuator) at the actuator center frequency were applied. Data were acquired at a sampling frequency of 20 MHz and 20 signals were averaged together. The fatigue cracks were initiated and grown by mechanical loading in a

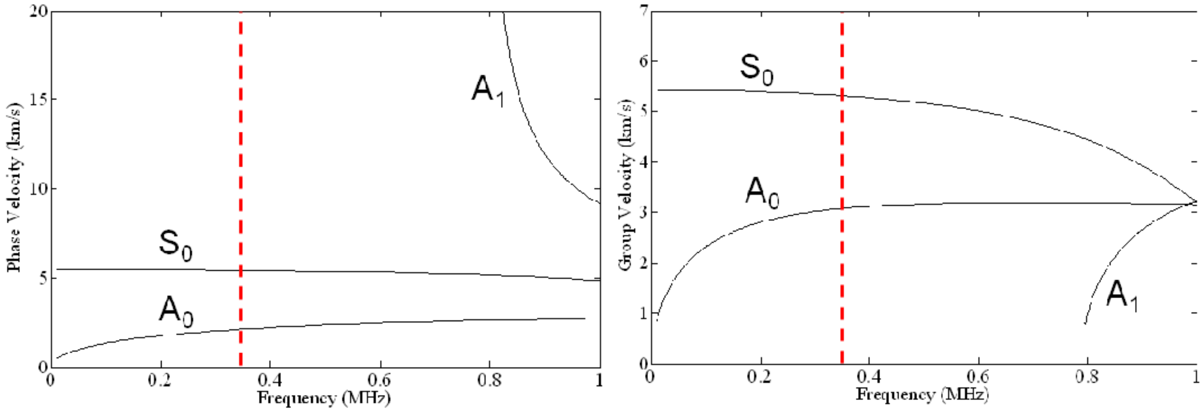

FIGURE 1. Phase and group velocity dispersion curves for a 2 mm thick aluminum plate with the 350 kHz central frequency of the transducers shown.

servohydraulic test machine (86 MPa maximum far field stress, 0.05 fatigue ratio, 5 Hz). No fatigue precrack was necessary, as the hole is a sufficient stress riser for crack initiation. The S0 group velocity was measured to be 5.24 mm/us, which compares very well with 5.26 mm/us obtained from the dispersion curves in Figure 1.

Training data is needed to locate and size a crack, so plates having 5 fastener holes spaced at 76 mm were fabricated. A linear array of 6 disk transducers was located on each side of the holes. Baseline signals were acquired (1 transmitter with 11 receivers times 12 = 132 paths) and then a 2 mm EDM slot was inserted on the left side of hole B (see Figure 2) and data acquired. The slot was then grown in 2 mm increments with data acquired after each increment. It is planned to acquire this type of training data from each possible crack initiation location. These sensor data enable creation of a tomogram to visualize the location of damage. Many signal features can be used in the RAPID algorithm [6]; here the signal difference coefficient is used. The RAPID algorithm is designed for damage anywhere within the region enclosed by the sensor arrays. In this application, the damage initiation lies along, or very close to, the centerline of the holes. Thus, the algorithm was revised from a family of ellipses to a family of concentric circles. The resulting tomogram is shown in Figure 2, where damage is correctly located on the left side of hole B.

The signal difference coefficient relies on a baseline. Others have shown [7] that environmental variables influence ultrasonic signals, thus the baseline for service conditions is expected to be correlated with temperature (by thermocouple), static load (by strain measurement), and fastener force (by pressure cell). A validated model to determine this baseline correlation will be needed.

In order to focus on detecting a small crack and be able to size it, a plate with a single hole is subjected to cyclic loading. Four transducers are mounted near the hole as shown in Figure 3. A sketch of the fatigue cracks that initiated at the hole is shown in Figure 4. The loading is in the vertical direction in both Figures 3 and 4 and the number of cycles used to grow the fatigue cracks to four specific lengths is given in Table 1. For each ID shown in Table 1 the cyclic loading was interrupted and guided wave monitoring performed. Monitoring was done both under zero applied load and under a static load equal to the maximum load during cycling (a far field stress of 86 MPa). Small fatigue cracks will close or partially close when the load is removed; thus it is important to characterize the difference in the guided wave features due to crack closure effects.

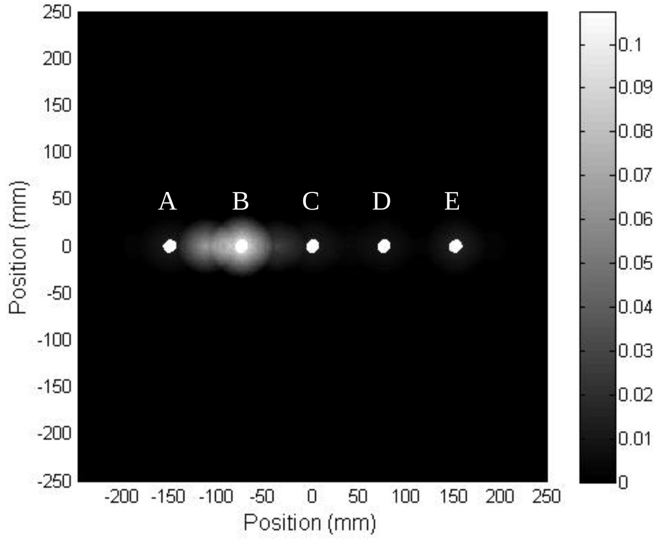

FIGURE 2. Tomogram showing location of 6 mm long EDM slot cut from left side of second 12.7 mm diameter hole.

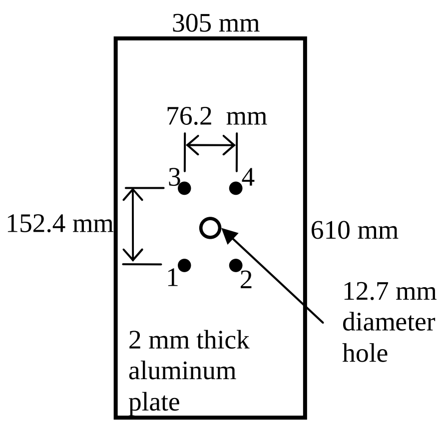

FIGURE 3. Transducer layout for single-hole plate sample.

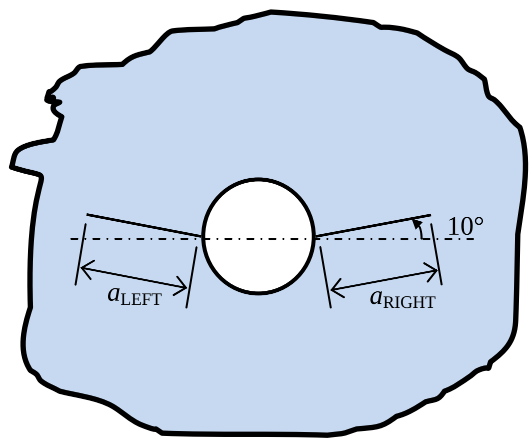

FIGURE 4. Schematic of fatigue crack growth from 12.7 mm diameter hole.

The initial signal received by transducer 4 (R4) that was transmitted by transducer 2 (T2) is shown in Figure 5. Time of flight calculations for S0 and A0 wave modes enable us to see that the first wave packet is the S0 mode, while the second wave packet is a combination of the A0 mode and edge reflections from the S0 mode. The expected arrival times for the S0 and A0 modes are marked with arrows along the top of Figure 5, where (1) is the arrival of the incident wave, (2) is arrival of a reflection from the hole, and (3) is arrival of a reflection from the edge of the plate. By taking the Hilbert transform of the received signal the positive envelope of the waveform can be obtained. The Hilbert transforms of the initial wave packet for wave propagation in the loading direction is shown in Figure 6 for four paths before crack initiation. Figure 6a signals are for zero load, while the signals shown in Figure 6b are obtained in the presence of static stress. The presence of a static stress appears to have a significant effect on the amplitude of the S0 wave packet, especially on the right side of the hole (T2-R4 and T4-R2). The difference between paths on the left side of the hole and those on the right side of the hole may be due to nonuniform load distribution. Table 1 shows that a crack on the right side of the hole initiated first. Unfortunately, no strain field measurements were made. Michaels et al [8] demonstrated the effect that static stress has on wave propagation. The data in Figure 6 show that a superimposed static stress component in the direction of wave propagation reduces the amplitude of the S0 mode, which is an in-plane mode. Analogous data is shown in Figure 7 for wave propagation transverse to the superimposed static stress. In this case the static stress has very little effect on wave propagation.

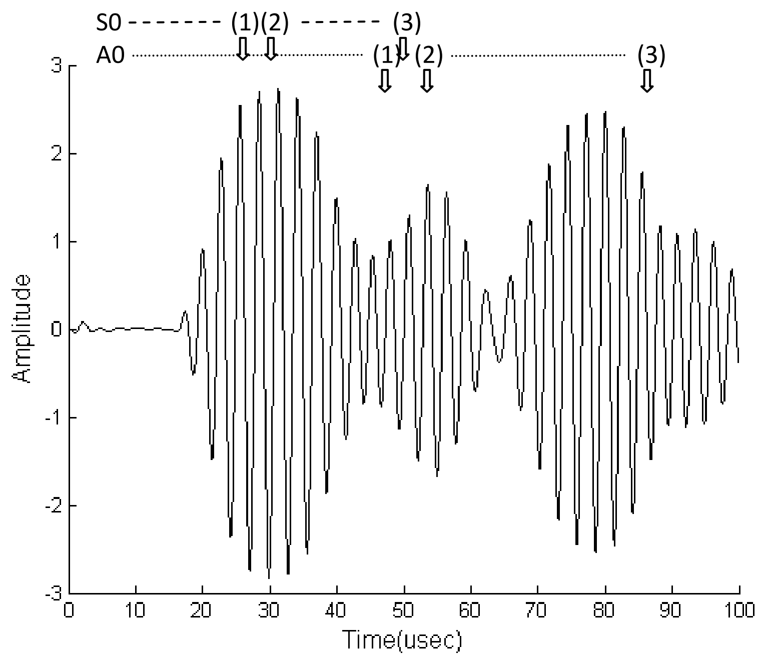

FIGURE 5. Initial A-scan (no load, no crack) for transducer path T2-R4 showing predicted arrival times for S0 and A0 wave modes.

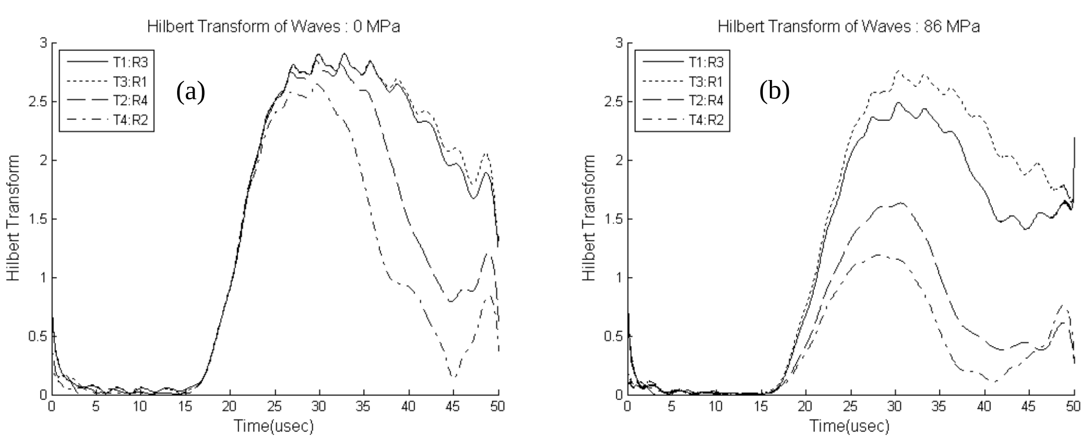

FIGURE 6. Hilbert transform of S0 mode signals; vertical wave propagation (a) unloaded, (b) 86 MPa far field static stress in vertical direction.

TABLE 1. Fatigue crack growth from 12.7 mm diameter hole.

ID	*N*, cycles	a_{LEFT}, mm	a_{RIGHT}, mm
N0	0	0.0	0.0
N1	46,839	0.0	1.7
N2	54,503	0.0	4.0
N3	64,489	0.0	8.0
N4	73,010	2.7	12.0

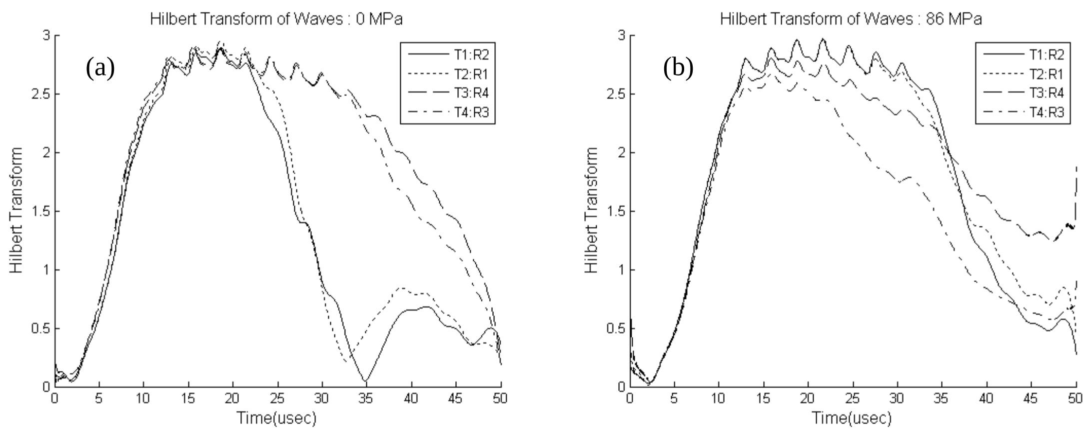

FIGURE 7. Hilbert transform of S0 mode signals; horizontal wave propagation (a) unloaded, (b) 86 MPa far field stress in vertical direction.

The Hilbert transforms of the signals from the T2-R4 path are shown in Figure 8 for zero load and 86 MPa and different crack lengths associated with IDs N0-N4 (see Table 1). Clearly, as the fatigue crack length increases the received signal amplitude becomes smaller, which suggests that the normalized S0 wave packet amplitude is a potential feature for sizing the fatigue crack. The baseline S0 amplitude (before loading) will be used to normalize the amplitude. Another potential feature is the signal difference coefficient (SDC),

$$SDC = 1 - \rho, \quad \rho = \frac{Cov(s_j, s_k)}{\sigma_{s_j} \sigma_{s_k}} \tag{2}$$

where ρ is the correlation coefficient, $Cov(s_j, s_k)$ is the covariance of the time domain signals s_j and s_k, and σ_s is the standard deviation. Here, j represents the baseline signal and k represents the current state signal. The SDC is zero for identical signals and it increases as the current state signal diverges from the baseline.

The results for stable crack growth are shown in Figure 9, where the normalized amplitude (Fig. 9a) and signal difference coefficient (Fig. 9b) are displayed as a function of the crack length, a_{RIGHT}. In both figures the results are from paths T2-R4 and T4-R2 for zero load and a static stress of 86 MPa. The normalized amplitude decreases significantly for a 1.7 mm crack for both zero load (partially closed crack) and in the presence of stress (partially open crack). The center excitation frequency is 350 kHz, which in an S0

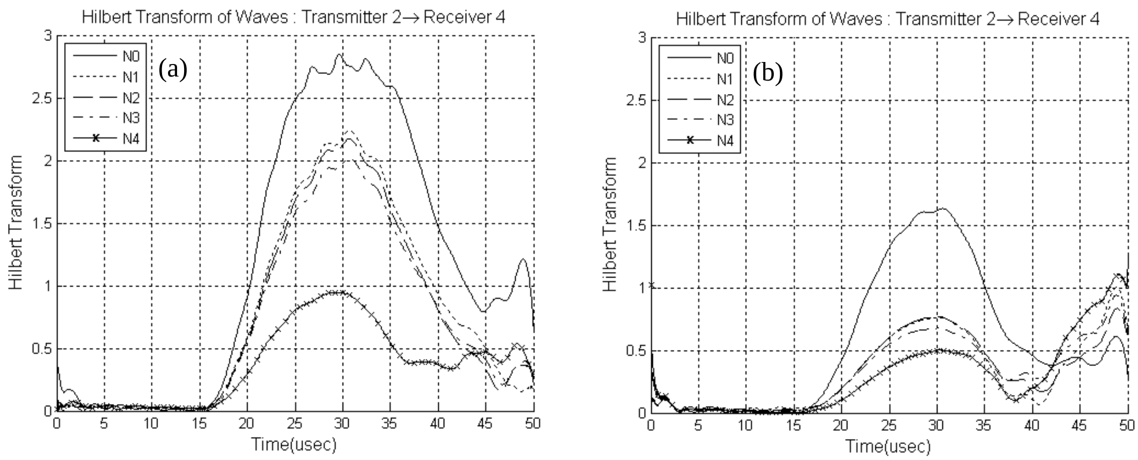

FIGURE 8. Fatigue crack effect on received signal (a) unloaded, (b) 86 MPa far field stress.

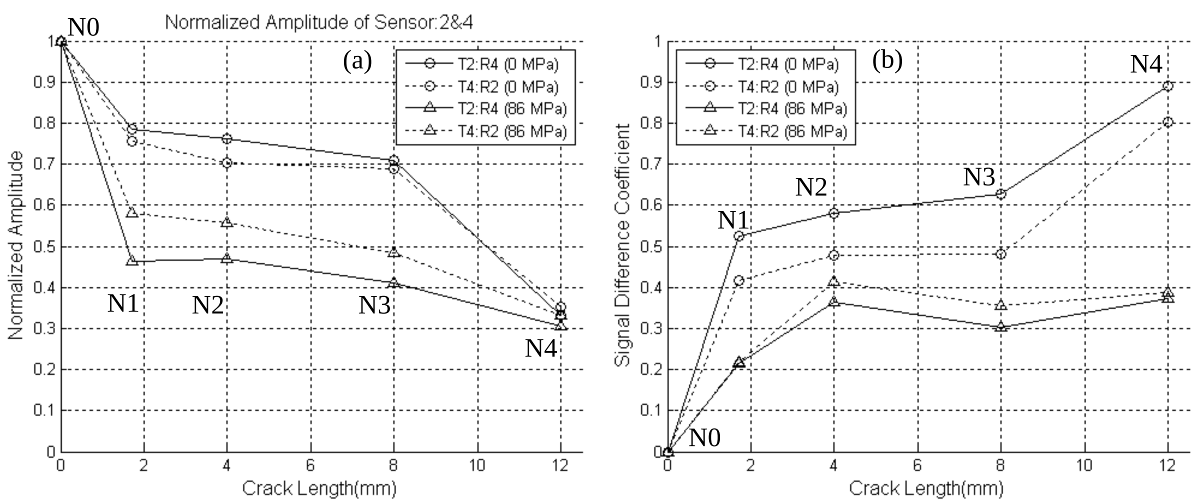

FIGURE 9. Effect of fatigue crack growth on (a) normalized amplitude of S0 mode, (b) signal difference coefficient for 20 < t < 40 us.

wavelength of 15 mm. Thus, the crack length is 1/9 of the wavelength. No attempt to acquire data for a smaller crack has been made yet. If plastic deformation occurs in the vicinity of the crack tip, crack closure is less likely to occur upon unloading. This could explain why the normalized amplitude curves converge in Fig. 9a for a 12 mm crack. The SDC for an unloaded crack increases continuously, but levels off at approximately 0.4 for a crack under stress. An explanation for the SDC saturating is under investigation.

CONCLUSION

Structural health monitoring of an aluminum joint structure using ultrasonic guided waves is being investigated. Some initial results have been presented herein. A tomography algorithm has been found to effectively detect and locate a small electric discharge machined slot in a cluster of fastener holes. The amplitude of the S0 Lamb wave mode appears to be sensitive to the presence of static stress in the direction of wave propagation. Both an amplitude ratio and the signal difference coefficient are sensitive to a fatigue crack emanating from a 12.7 mm diameter fastener hole. The smallest fatigue crack investigated to date is 1.7 mm, which is evident from the signal of the S0 mode that has a wavelength of 15 mm.

ACKNOWLEDGEMENTS

This work is supported by the Ben Franklin Center of Excellence in Structural Health Monitoring.

REFERENCES

1. F. Yan, "Ultrasonic guided wave phased array for isotropic and anisotropic plates," Ph.D. Thesis, The Pennsylvania State University (2008).
2. R.L. Royer, X. Zhao, S.E. Owens, and J.L. Rose, "Large area corrosion detection in complex aircraft components using Lamb wave tomography," in *Structural Health Monitoring 2007*, edited by F.K. Chang, Destech Publications, Lancaster, PA (2007), pp. 238-246.
3. K. Worden, C.R. Farrar, G. Manson, and G. Park, "The fundamental axioms of structural health monitoring," *Proc. Roy. Soc.* **A463**, pp. 1639-1664 (2007).
4. S.S. Kulkarni and J.D. Achenbach, "Structural health monitoring and damage prognosis in fatigue," *Struct. Health Mon*. **7**, pp. 37-49 (2008).
5. A.C. Cobb, J.E. Michaels, and T.E. Michaels, "Ultrasonic structural health monitoring: a probability of detection case study," in Review of Progress in QNDE, 28A, edited by D.O. Thompson and D.E. Chimenti, AIP Conference Proceedings vol. 1096, American Institute of Physics, Melville, NY (2008), pp. 1800-1807.
6. T.R. Hay, R.L. Royer, H. Gao, X. Zhao, and J.L. Rose, "A comparison of embedded sensor Lamb wave ultrasonic tomography approaches for material loss detection," *Smart Mater. Struct*. **15**, pp. 946-951 (2006).
7. G. Manson, "Identifying damage sensitive environment insensitive features for damage detection," in *Proc. Int. Conf. on Identification in Engineering Systems*, Swansea, UK, pp. 187-197 (2002).
8. J.E. Michaels, T.E. Michaels, R.S. Martin, "Analysis of global ultrasonic sensor data from a full scale wing panel test," in Review of Progress in QNDE, 28A, edited by D.O. Thompson and D.E. Chimenti, AIP Conference Proceedings vol. 1096, American Institute of Physics, Melville, NY (2008), pp. 950-957.